



## Research Article

# Experimental and numerical study for assessment indoor air quality by adopting mixing ventilation with different occupants' density in Iraq hot climates

Atheer Hmaizah SABR<sup>1,\*</sup>, Alaa Abbas MAHDI<sup>2</sup>, Mohammed Wahhab ALJIBORY<sup>1</sup>

<sup>1</sup>College of Engineering, Kerbala University, 56001, Iraq

<sup>2</sup>College of Engineering, Babylon University, 51002, Iraq

## ARTICLE INFO

### Article history

Received: 05 July 2022

Revised: 16 January 2023

Accepted: 08 February 2023

### Keywords:

Computational Fluid-Dynamics (CFD); Indoor Air Quality (IAQ); Mixing Ventilation (MV); Thermal COMfort; Occupied Density

## ABSTRACT

In this research, thermal of level comfort and air quality indoor were examined for different numbers of persons (occupants' density) within a (3m × 2.5m × 2.5 m) office room. The office room is equipped with mixing ventilation system, temperature and air speed (17°C) and (2.5 m/s) respectively. The results of experimental experiments and results were compared with computational fluid- dynamics (CFD) analysis utilizing the turbulent (RNG, k-epsilon) model on a thermal manikin that represents a person's body in a standing and sitting and position. The experimental study focused on measuring the velocity, air temperature, and carbon dioxide (CO<sub>2</sub>) concentration in different areas indoor the room, in addition to taking measurements around the heat manikins and in the breathing area. When analyzing numerical data, thermal of level comfort was assessed by air diffusion of performance Index (ADPI), predicted of percentage dissatisfied (PPD), and predicted of mean vote (PMV). The results indicate that thermal comfort and indoor air quality decline with more persons. Where the values of (ADPI), (PPD) and (PMV) change from (76.55 %), (6.325 %) and (0.021) to (64.25 %), (10.412 %) and (0.52) respectively, when the number of persons in the room increased from (two persons) to (four persons).

**Cite this article as:** Sabr AH, Mahdi AA, Aljibory MW. Experimental and numerical study for assessment indoor air quality by adopting mixing ventilation with different occupants' density in Iraq hot climates. J Ther Eng 2024;10(2):430–446.

## INTRODUCTION

Air conditioning systems, or standalone air conditioners, provide cool, ventilate, and control humidity for all parts of the home or building. In enclosed spaces, ventilation is one

of the essential methods used to control indoor air quality (IAQ). In buildings, ventilation has an impact on the structure and, as a result, on the people who utilize it. Ventilation is the process of changing and replacing air (remove old air and insert fresh air instead). As the ventilation controls and

### \*Corresponding author.

\*E-mail address: [Atheer.h@s.uokerbala.edu.iq](mailto:Atheer.h@s.uokerbala.edu.iq)

This paper was recommended for publication in revised form by Regional Editor Tolga Taner



regulates the temperatures inside the rooms, as well as eliminating unpleasant odors and harmful gases and controlling the level of humidity inside the building.

A deteriorated indoor environment increases sick building syndrome (SBS), respiratory illnesses, and reduces comfort and productivity. To obtain an excellent indoor environment that meets human physiological and health needs, as well as provide some kind of luxury. Good ventilation system inside buildings, homes, and offices is needed. The function of a ventilation system is not limited to providing the building with oxygen only but also for the disposal of carbon dioxide [1].

Improvement of the indoor environment is economically efficient when health and productivity are taken into account. A group of field studies conducted showed, significant levels of dissatisfaction with the indoor environment in many buildings despite satisfying the typical ventilation requirements, where there are still many complaints regarding poor indoor air quality and diseases related to poor ventilation of buildings [2].

There are significant individual differences among occupants regarding the physiological and response of psychological, activity, temperature of air, and preference of air movement, etc. Therefore, a unique set of thermal parameters (i.e., temperature of air, average radiating temperature, relative humidity and velocity of air) is unable to meet everyone's requirements. The rate of ventilation must be recognized in order to accomplish optimum ventilation (the rate of ventilation is the number of times in one hour that one cubic meter of air in a place has to be refreshed) (ACH) and this is dependent on the volume and area of the space, the function of the building, the number of inhabitants in the space, and heat and moisture sources both outside and inside the space [3].

Mixing ventilation is system that combines the supply air with the room's old air to maintain the same design temperature inside the room [4]. The air velocity is high so that the air stream leads to disturbance, which leads to mixing the air of room with the supply air. The entire room is thoroughly mixed, so small temperature difference, and the concentration of pollutant is uniform throughout the room. In this type, air diffusers are usually used as an air outlet for high-speed air current, where most of the air outlets and inlets are installed near the roof in the upper part of the wall outside the occupied zone. In mixing ventilation system, the air supply is usually done at speed ranging between (2 – 8) m/s and a temperature of (9 – 40) °C [5].

Glenn et. al. (2011) [6], examined a ventilation system in a laboratory with dimensions of (6×3×3.5) m. Simulation has been done Using (ANSYS FLUENT 12.1.1) the program in which the (RNG k- $\epsilon$ ) model is implemented [7]. The focus of the simulation was on the effect of changing the air flow rate to remove spilled pollutants. The results indicated that the best design should not only depend on changing the air flow rate, but should also depend on the density and activity of the occupants. Xue et al. (2020) [8],

investigated experimental in a surgical suite with mixing ventilation, researchers looked at the impact exhaust airflows on the surgical environment. Temperature, air speed, humidity, and indoor quality are all factors that must be met in the indoor environment. The research was conducted in a full-size of operating room laboratory (8 × 7 × 3.8) m, in Trondheim, Norway, at the Norwegian University of Science and Technology. According to the findings, the ideal location for the instrument table is (1.0–1.5 m) from the wall. Shah et al. (2021) [9], studied in the context of COVID-19, an experimental assessment of indoor aerosol dispersion and buildup was conducted, including the effects of ventilation and masks. According to measurements, every mask put to the test offers protection to the host's immediate area, mostly via deflecting and reducing expiratory momentum. Even with high-efficiency of masks like the (KN95 or R95), When compared to the material's ideal filtration efficiency, leakages are seen to cause noticeably reduced mask efficiency. Tests conducted at a distance of (2 m) from the subject show a significant increase of aerosols with time in the interior environment (10 h). Larger ventilation capacity is necessary to completely reduce aerosol build-up, but the findings show that even low air-change rates (2 per hour) result in reduced aerosol build-up when compared to the best mask in an unventilated room.

The aims of this research are to see how increasing the number of persons (occupants' density) in a room affects indoor air quality and thermal comfort. To investigate Air Diffusion Performance (ADPI), Predicted of Mean Vote (PMV) and Predicted of Percentage Dissatisfied (PPD) by CFD modeling by ventilation the room under the Iraqi climate. Matching numerical results to experimental results, evaluating those results' accuracy, and then comparing those results to those of experiments carried out on real persons.

## EXPERIMENTAL METHOD

The material (Sandwich panel) was utilized to build a room that is (3 × 2.5 × 2.5) m in size and thermally insulated. These tests were carried out in the laboratories of the University of Babylon's Faculty of Engineering in the Iraqi city of Babylon. Both experimental and numerical analysis assumed steady-state working conditions. The temperature distribution and carbon dioxide distribution (CO<sub>2</sub>) surrounding persons and indoor the room were calculated in practical studies, as were the rates of airflow, temperature and speed at the air diffuser mixing ventilation (MV device). The test room contained a variety of heat sources, including two boxes with heat sources that resembled computers (75 Watt), thermal manikins that produce sensible heat (80 Watt per thermal manikin), and one light bulb (100 Watt). as shown in Figures 1, 2, 3, 4 and 5. Table 1 lists the distribution and positioning of the individuals and objects in the room. The chilled air was delivered to the room's indoor space using a commercial air conditioner.

Table 1. Isolated test room contents

Item	Location (m)						Sensible Heat (W) [10]
	Start			End			
	(X)	(Y)	(Z)	(X)	(Y)	(Z)	
Office room	0.0	0.0	0.0	3.0	2.50	2.50	
Mixing device	0.0	2.10	1.15	0.10	2.20	1.35	
Exhaust air grille	0.0	0.30	1.17	0.0	0.40	1.33	
Person no. (1)	0.15	0.0	0.30	0.35	1.10	0.70	80
Person no. (2)	2.65	0.0	1.80	2.85	1.10	2.20	80
Laptop no. (1)	0.60	0.76	0.35	0.90	1.06	0.65	75
Laptop no. (2)	2.10	0.76	1.85	2.40	1.06	2.15	75
Lamp (light)	1.45	2.40	2.30	1.55	2.45	2.50	170
COmputer disk no.1	0.50	0.76	0.0	1.0	0.0	1.0	
COmputer disk no.2	2.0	0.76	1.50	2.50	0.0	2.50	

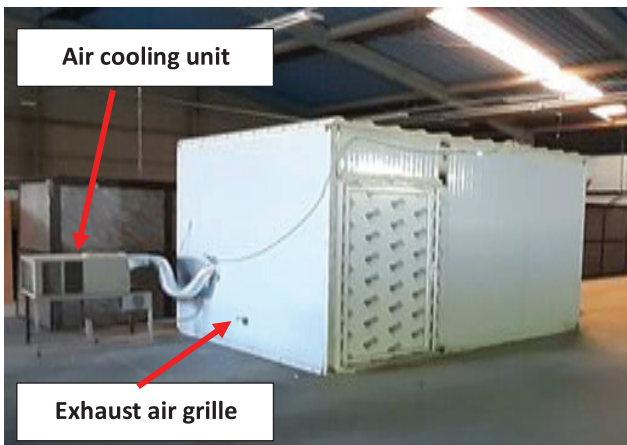


Figure 1. Experimental room from outside.

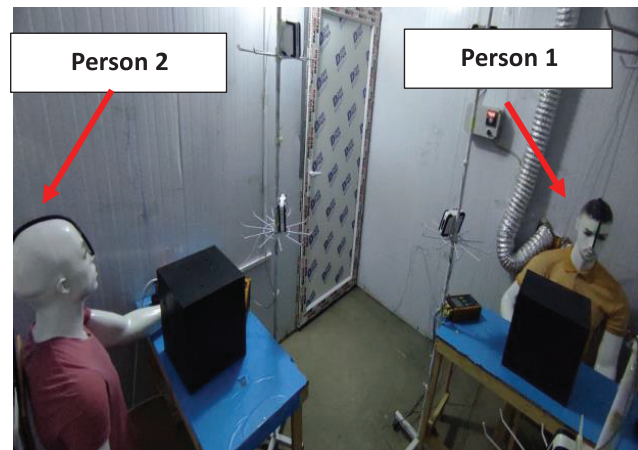


Figure 2. Experimental room (case I).

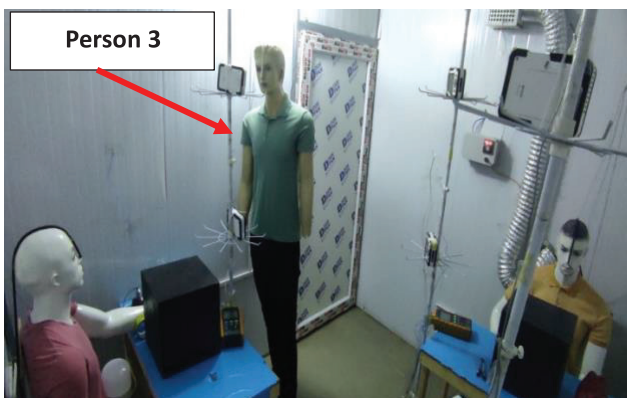


Figure 3. Experimental room (case II).

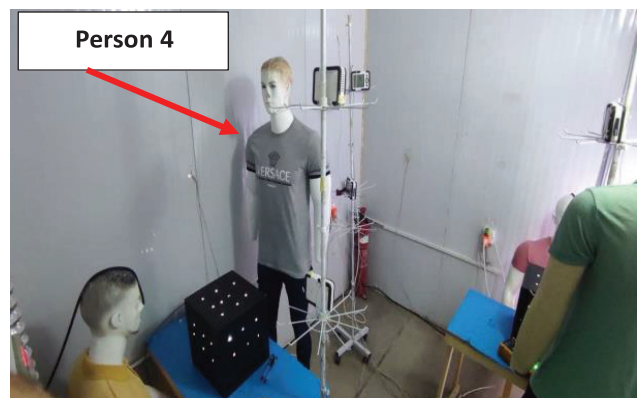


Figure 4. Experimental room (case III).

The manikin generates carbon dioxide (CO<sub>2</sub>) by placing a source of carbon dioxide in the room and connecting a thin tube to manikin nose.

The indoor air conditions for office room design as dry bulb temperature (T<sub>dr</sub>) of (25 °C due to ASHRAE.2012) [11]. For mixing ventilation, the different temperature between

head and foot for occupant ( $\Delta T_{hr}$ ) is (2 °C) for seated person and (3 °C) for standing person due to ASHRAE Standard 55, [12].

**Supply Air System**

Air was provided at speeds between (2.5 and 8) m/s and temperatures between (15 and 22 °C). The diffuser’s supply air should flow at a temperature and speed of (17 °C) and (2.5 m/s), respectively, that have been determined through testing and research. The supply ventilation rate for mixing ventilation (MV) systems and total heat applications is calculated using the two techniques shown below, (Awbi, 2017) [13]. The required air volume (airflow rate) is estimated, and the formulas below are used to determine the heat transfer resulting from the ventilation process:

$$Q_{total} = \dot{m} \times cp \times \Delta T \tag{1}$$

$$Q_{total} = q_{oe} + q_1 + q_{ex} \tag{2}$$

The design airflow rate (l/s) in the equations above can be determined from the value of the mass flow rate ( $\dot{m}$ ).

$$Q_s = \frac{\dot{m}}{\rho} \tag{3}$$

The air was delivered at a rate of (2.5 m/s). Equation (4) was used to calculate the cross-sectional area of the air diffuser.

**Procedures for Experimental**

A group of experiments was conducted in May and June 2022, and there were three cases of experiments, according to the number of persons (occupants’ density). The first case involves the use of only two persons. The second case uses three persons and the third case uses four persons. After two hours of operation, the system has nearly stabilized, all ventilation measurements were taken in terms of temperature distribution and carbon dioxide concentration (CO<sub>2</sub>) within the room, each experiment was carried out five times, and the most precise findings were obtained by averaging the values.

$$Q_s = U_x \times A_s \tag{4}$$

Where:

( $U_x$ ): local air speed (m/s)

( $A_s$ ): Air supply diffuser’s surface area (m<sup>2</sup>).

Then  $A_s = 0.05/2.5 = 0.020$  m<sup>2</sup>.

**Description of Case Study**

The steady state experiments aim to investigate the mixing ventilation based on occupied density in a steady state and reported sets of temperature distribution, carbon dioxide concentration and thermal comfort parameters. The operating conditions of the (MV) system in the test office room are:

1. The air flow rate is fixed at 50 l/s.
2. The air velocity of mixing diffuser is 2.5 m/s (constant for all the cases).
3. The supply temperature of the diffuser 17 °C (constant for all the cases).

A series of three cases were completed with the (MV) system operating. Table 2 shows a description for each case.

**Initial Conditions**

Table 3 shows the ambient temperature, relative humidity (RH) and the carbon dioxide concentration (CO<sub>2</sub>) on the test day under the climate of Hilla – Iraq.

**Measurement Devices**

There are 24 thermocouples (K-Type) which connected to two data temperature recorder (BTM4208 SD) systems Figure (5a), each supporting 12 channels. Type (k) of thermocouples have a good accuracy of ( $\pm 0.1$  °C).

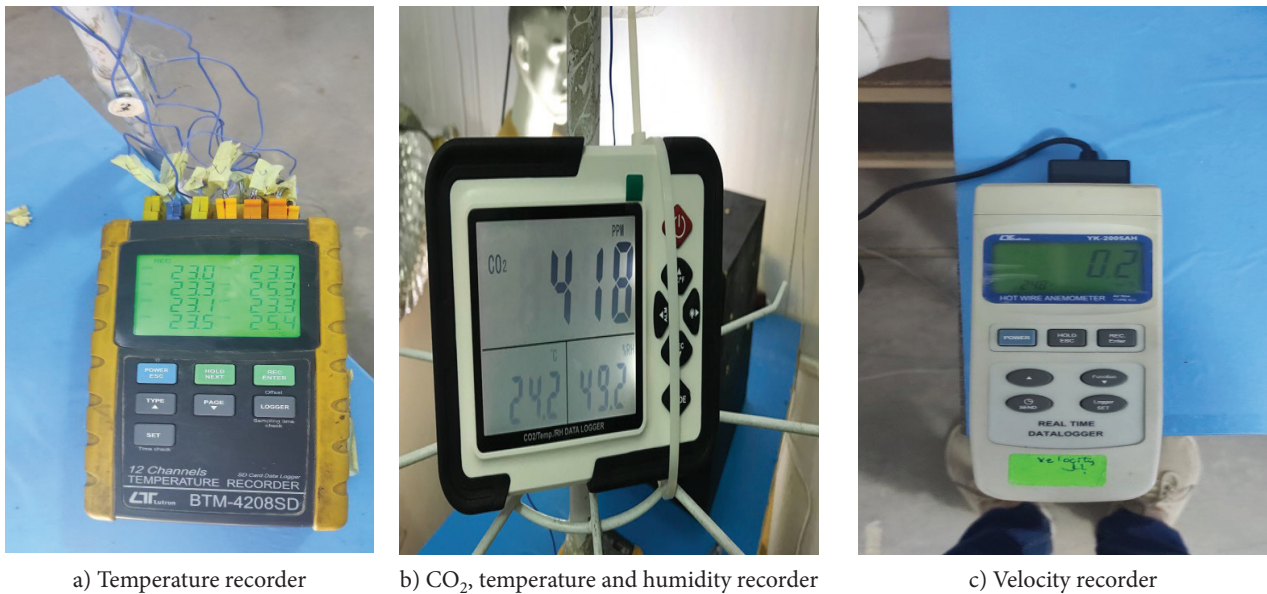
During experiment tests, 4 thermocouples were placed on side walls (one thermocouple at each wall). Eight thermocouples were placed on persons and 12 thermocouples fixed on the three stands to measure air temperature distribution with high. CO<sub>2</sub> concentration and humidity measurement system is based on a set of CO<sub>2</sub> and humidity recorder devices Figure (5b). Fixed at six points in different locations of test room at breathing zoon for the sitting and

**Table 2.** Description of the cases

Cases	Occupants density (Persons)	Air flow rate	
		l/s	cfm
I	2	50	105
II	3	50	105
III	4	50	105

**Table 3.** Ambient temperature, CO<sub>2</sub> concentration and relative humidity at test days

Case	Experimental day	Tamb °C	RH%	CO <sub>2</sub> (ppm) concentration
I	30/5/2022	41.5	30	488
II	3/6/2022	41	31	486
III	6/6/2022	42.5	28	484



a) Temperature recorder      b) CO<sub>2</sub>, temperature and humidity recorder      c) Velocity recorder

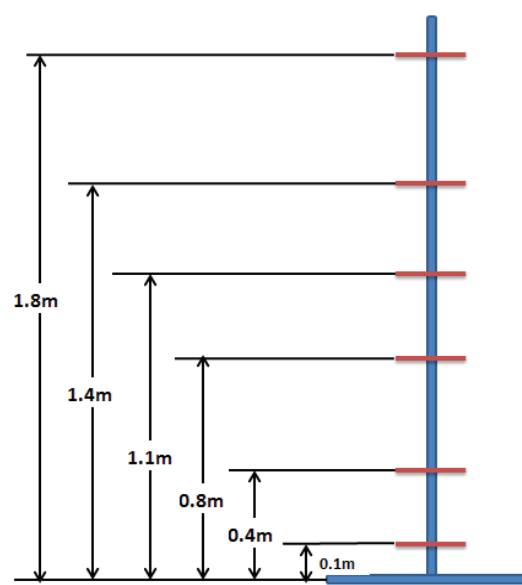
**Figure 5.** Measurement devices.

standing person (1.1 m) and (1.8 m) respectively. Supply velocity was measured by thermos-anemometer device, Figure 5c.

**Description and Arrangement Measurement Devices**

Three vertical stands are placed in test room. Each stand has six levels from (0.1 to 1.8) m as show in Figure 6. These stands carried thermocouples, (CO<sub>2</sub>) measurement and humidity devices to cover environment in occupied zone.

The stands are placed inside the tested chamber in three locations as shown in Figure 7. The first electrode (stand-1) is located near the supply distributor and the other electrode (stand-2) is placed in front of the heat dwarf and (stand-3) in the region far from persons. The air that enters the chamber is labeled with a trace gas, and the concentration of this trace gas is measured at the site of interest. This assumes that the behavior of the trace gas is the same as that of air. This method gives a good idea of the efficiency of the



a- Photograph of stands

b- Schematic diagram of stand

**Figure 6.** Distribution of the measurement devices on a stand.

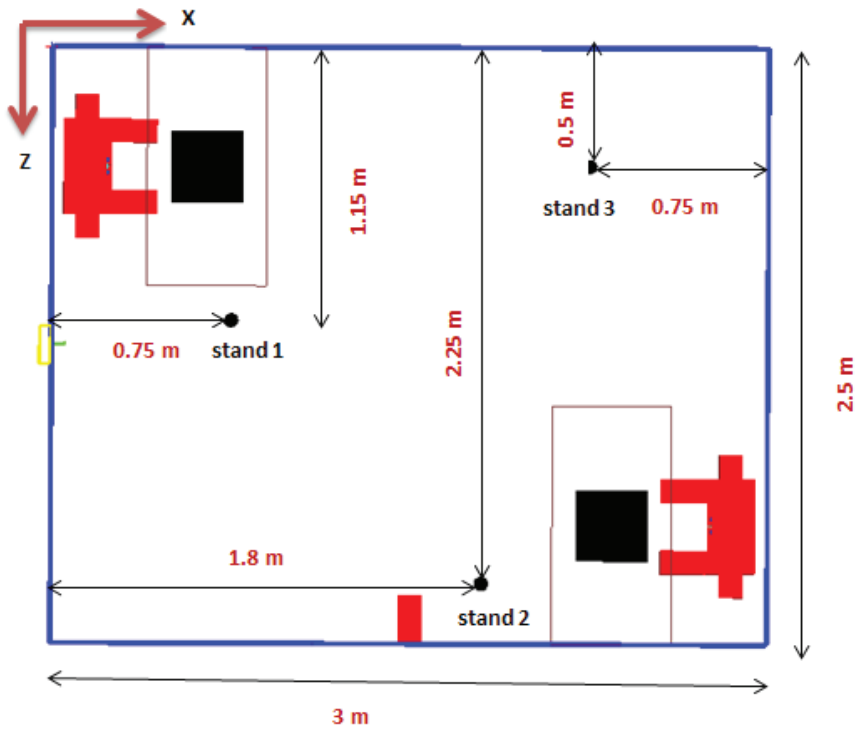


Figure 7. Locations of the measurement stands.

system in removing contaminants. The temperature distribution with altitude is measured in the case of the study. Figure 7 Locations of the measurement stands

**NUMERICAL METHOD**

A room has been numerically simulated with its dimensions (3×2.5×2.5m) (x×y×z) using (ANSYS 15.0) [19] and

the use of turbulence model (RNG-k-ε), as well as simulating its occupants and contents shown in the Table 1 and Figure 8.

The flow was classified as a stable, three-dimensional, Newtonian, incompressible fluid with no chemical reaction, as well as a turbulent flow fluid, ideal fluid, and frictionless fluid. in the current study based on CFD simulation (Awabi, 2017) [13].

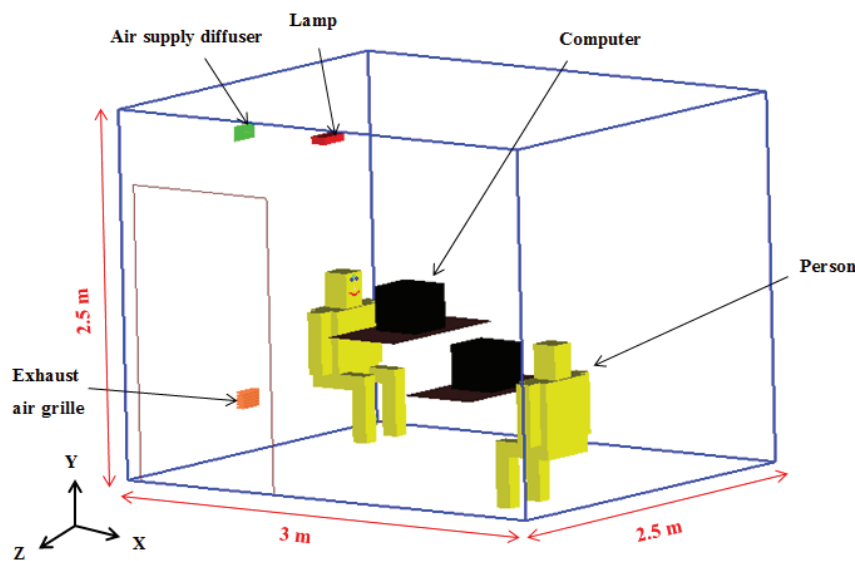


Figure 8. Schematic drawing of the office room.

### General Governing Equations [13]

$$\frac{\partial}{\partial x}(\rho u) + \frac{\partial}{\partial y}(\rho v) + \frac{\partial}{\partial z}(\rho w) = 0 \quad (5)$$

$$\begin{aligned} \frac{\partial}{\partial x}(\rho uu) + \frac{\partial}{\partial y}(\rho uv) + \frac{\partial}{\partial z}(\rho uw) &= -\frac{\partial p}{\partial x} + \frac{\partial}{\partial x}\left(\mu \frac{\partial u}{\partial x}\right) \\ &+ \frac{\partial}{\partial y}\left(\mu \frac{\partial u}{\partial y}\right) + \frac{\partial}{\partial z}\left(\mu \frac{\partial u}{\partial z}\right) + \frac{1}{3} \frac{\partial}{\partial x}\left[\mu \left(\frac{\partial u}{\partial x} + \frac{\partial v}{\partial y} + \frac{\partial w}{\partial z}\right)\right] \\ &+ \frac{\partial}{\partial x}(-\rho \overline{u'u'}) + \frac{\partial}{\partial y}(-\rho \overline{u'v'}) + \frac{\partial}{\partial z}(-\rho \overline{u'w'}) + \rho g_x \end{aligned} \quad (6)$$

$$\begin{aligned} \frac{\partial}{\partial x}(\rho uv) + \frac{\partial}{\partial y}(\rho vv) + \frac{\partial}{\partial z}(\rho vw) &= -\frac{\partial p}{\partial y} + \frac{\partial}{\partial x}\left(\mu \frac{\partial v}{\partial x}\right) \\ &+ \frac{\partial}{\partial y}\left(\mu \frac{\partial v}{\partial y}\right) + \frac{\partial}{\partial z}\left(\mu \frac{\partial v}{\partial z}\right) + \frac{1}{3} \frac{\partial}{\partial y}\left[\mu \left(\frac{\partial u}{\partial x} + \frac{\partial v}{\partial y} + \frac{\partial w}{\partial z}\right)\right] \\ &+ \frac{\partial}{\partial x}(-\rho \overline{u'v'}) + \frac{\partial}{\partial y}(-\rho \overline{v'v'}) + \frac{\partial}{\partial z}(-\rho \overline{v'w'}) + \rho g_y \end{aligned} \quad (7)$$

$$\begin{aligned} \frac{\partial}{\partial x}(\rho uw) + \frac{\partial}{\partial y}(\rho vw) + \frac{\partial}{\partial z}(\rho ww) &= -\frac{\partial p}{\partial z} + \frac{\partial}{\partial x}\left(\mu \frac{\partial w}{\partial x}\right) \\ &+ \frac{\partial}{\partial y}\left(\mu \frac{\partial w}{\partial y}\right) + \frac{\partial}{\partial z}\left(\mu \frac{\partial w}{\partial z}\right) + \frac{1}{3} \frac{\partial}{\partial z}\left[\mu \left(\frac{\partial u}{\partial x} + \frac{\partial v}{\partial y} + \frac{\partial w}{\partial z}\right)\right] \\ &+ \frac{\partial}{\partial x}(-\rho \overline{u'w'}) + \frac{\partial}{\partial y}(-\rho \overline{v'w'}) + \frac{\partial}{\partial z}(-\rho \overline{w'w'}) + \rho g_z \end{aligned} \quad (8)$$

Where the terms  $(\rho \overline{u'w'}, -\rho \overline{w'w'}, \rho \overline{u'v'}, \rho \overline{v'w'}, \rho \overline{u'w'})$  are the turbulent Reynolds shear stress ( $\tau_t$ ) and  $(\rho g_{x,y,z})$  is body force.

$$\begin{aligned} \frac{\partial(\rho \overline{u_i u_j})}{\partial t} + \frac{\partial(\rho V_k \overline{u_i u_j})}{\partial x_k} &= P_{ij} - \frac{2}{3} \delta_{i,j} \rho \varepsilon + \Phi_{ij} \\ &+ P_{ij,b} + \frac{\partial}{\partial x_k} \left( \mu + \frac{2}{3} C_s \rho \frac{k^2}{\varepsilon} \right) \frac{\partial \overline{u_i u_j}}{\partial x_k} \end{aligned} \quad (9)$$

### Parameters of the Numerical Study

#### Predicted mean vote (PMV)

The (PMV) value is graded on a seven-point scale, ranging from +3 for chilly indoor air to -3 for hot indoor air. The best range of (PMV) for acceptable internal comfort, according to (ASHRAE standards), is  $(-0.5 < \text{PMV} < 0.5)$  [15,17,21].

#### Predicted percentage dissatisfied (PPD)

(PPD) estimates the percentage of persons experiencing extreme heat or cold. (PPD), computed from the expected mean vote (PMV). According to  $(-0.5 < \text{PMV} < 0.5)$ , the usual limit of PPD for a good thermal environment is (10%) [15,17,21].

#### Air diffusion performance index (ADPI)

Air temperature and velocity are measured at uniformly spaced points within the occupied zone or through a vertical centerline plane through the air supply outlet. The lowest value of (EDT) is equal to  $(-1.7 \text{ }^\circ\text{C})$ , while the highest value is  $(1.1 \text{ }^\circ\text{C})$ . As for air velocity, it is taken equal to  $(0.25 \text{ m/s})$  [15].

#### Mash Strategy

The FLUENT CFD engine is used by the numerical simulation program ANSYS 15.0 to solve thermal calculations and the equation to conserve mass, energy, and air momentum. To solve flow equations, the (RNG, K- $\varepsilon$ ) turbulence model was employed. In this study, in this study, hexa unstructured geometry was employed to discretize. Simulations were run until the results were stable to a level of approximation (10-3), as shown in the Figure 9. A mesh improvement research was also undertaken to detect and reduce the estimation inaccuracy. To conduct the test, four distinct mesh systems were created: coarser type, course type, medium type, and fine type (Jassem et al., 2019) [16].

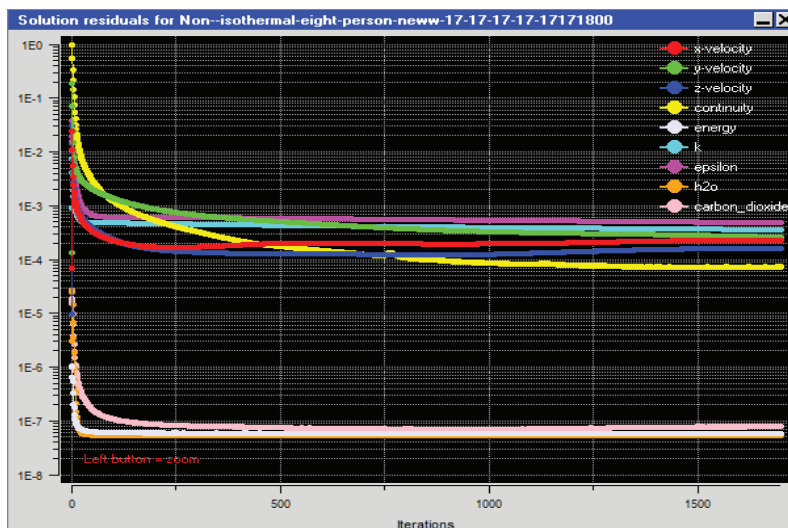


Figure 9. Plot of residuals.

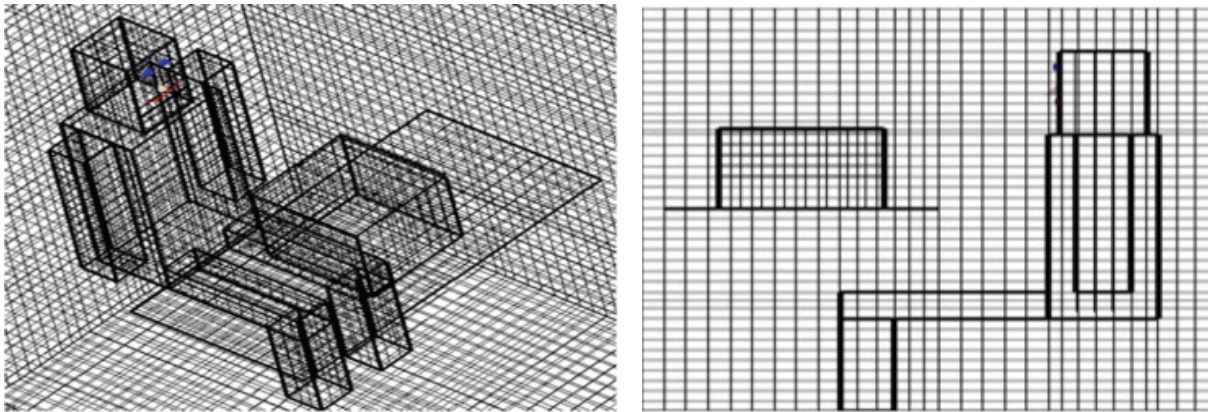


Figure 10. A portion of the mesh model.

Table 4. Mesh strategy

Test room	Case	Persons No.	Element No.	Node No.
	I	2	598115	623878
	II	3	688358	719048
	III	4	841250	879265

The model was created with ANSYS 15.0, [19] software, and study cases were meshes based on various testing meshes, as shown in Figure 10, the dimensions of room edges in (x, y, z) mesh as (0.04) interval size, mesh parameter normal, and max side ratio (2). After implementing the meshing approach, the choice was made after numerous trials as listed in Table 4.

## RESULTS AND DISCUSSION

### Experimental Results

#### Temperature distribution analysis

The diffuser (MV) device, which is located in the middle of the north side wall, provides high-speed air with a

speed and temperature of (2.5 m/s) and (17 °C), respectively. Six different heights were employed to measure the temperature inside the room on three stands in each stand (0.1 - 1.8) m, the relationship between air temperature and height for three poles is shown in Figure 11. The temperature of the air was of measured at various altitudes, as listed in Table 5.

The distribution of temperature is uniform according to the experimental findings. The supply of air with a high speed and momentum is the cause for the uniform distribution of temperature inside the room. Thus, the movement of particles is affected by the density difference between cold and hot air. Where it is noted that the highest temperature inside the room is at the lowest levels due to the heat sources and the location of the air distributor at the top. The upper layers of the room are affected by cold air supply, and

Table 5. Experimental measurements data for the case I

Height	1 <sup>st</sup> stand	2 <sup>nd</sup> stand	3 <sup>rd</sup> stand
m	Temperature °C	Temperature °C	Temperature °C
0.1	24.2	24.532	24.752
0.4	24.335	24.841	24.791
0.8	24.435	24.934	24.93
1.1	24.483	25.21	25.351
1.4	24.532	25.635	25.447
1.8	24.631	25.937	25.631

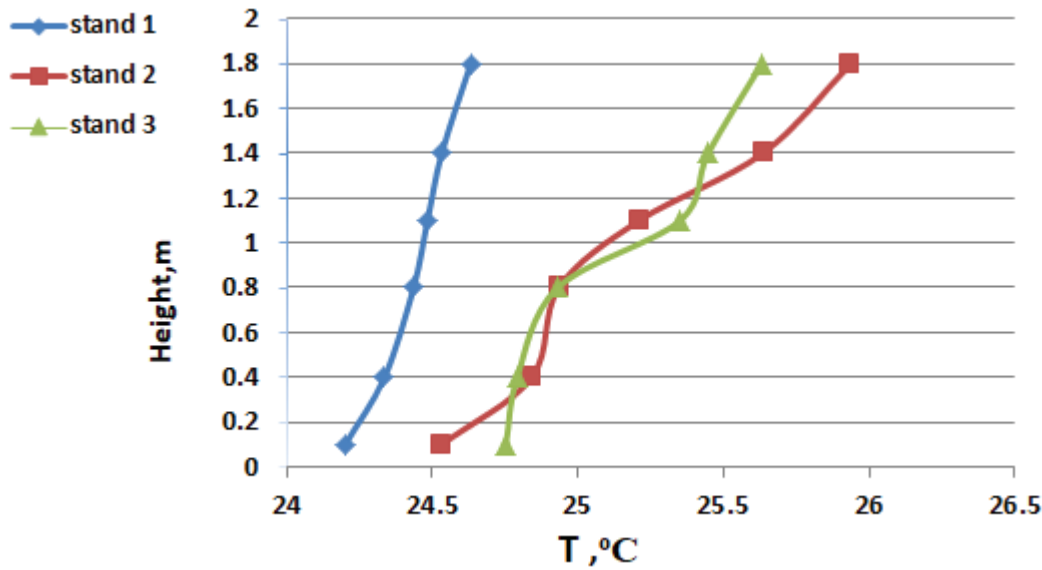


Figure 11. Temperature distribution (case I).

therefore its temperature decreases and its density increases to bring the molecules closer and thus decreases to the bottom to be replaced by hot air due to its low density, and this process is repeated for several times in order to reach the design temperature (25 °C).

In this case (II), occupant's density increases to (Three persons). Figure 12 Table 6, shows the measurement of temperatures at the same heights and different locations of the stands.

The increase in room temperature was observed in general when changing the density of the occupants from ( two persons ) to (three persons), and the reason for this increase in temperature is due to the addition of a heat source (third person) as the person according to the source ASHRAE gives ( 80 W). The highest of temperature in the room was near the floor begins to fall with increasing height. The air velocity and temperature of the breathing area (1.1 m) in sitting and breathing area (1.8 m) in standing were measured, and it was noted that the temperature was acceptable

and not as good as in the first case. As for the air velocity in the breathing areas, it didn't go faster than (0.25 m/s), and is considered suitable for thermal of level comfort.

In this case (III), occupant's density increases to (Four persons). Experimental temperature data are shown in Table 7.

The relationship between temperature and height across the stands is depicted in Figure 14 (1,2 and 3). In general, high temperatures were observed at all points specified on the three stands. The temperature distribution became less uniform, indicating lower indoor air of quality (IAQ) and thermal level of comfort indoor the test room. The subjects' temperatures were discovered to be higher than in previous cases, which is not good.

#### Analysis of carbon dioxide concentrations (CO<sub>2</sub>)

Figures 15 and 16 are the current measured mean of (CO<sub>2</sub>) concentrations at two levels of altitude for the sitting and standing breathing area for three cases, respectively, at where (a) at the (1.1 m) altitude level and (b) at the 1.8 m

Table 6. Experimental measurements data for the case II

Height m	1 <sup>st</sup> stand	2 <sup>nd</sup> stand	3 <sup>rd</sup> stand
	Temperature °C	Temperature °C	Temperature °C
0.1	24.73	25.23	25.42
0.4	25.01	25.45	25.53
0.8	25.21	25.67	25.66
1.1	25.33	25.761	25.83
1.4	25.631	25.96	26.15
1.8	25.75	26.27	26.43

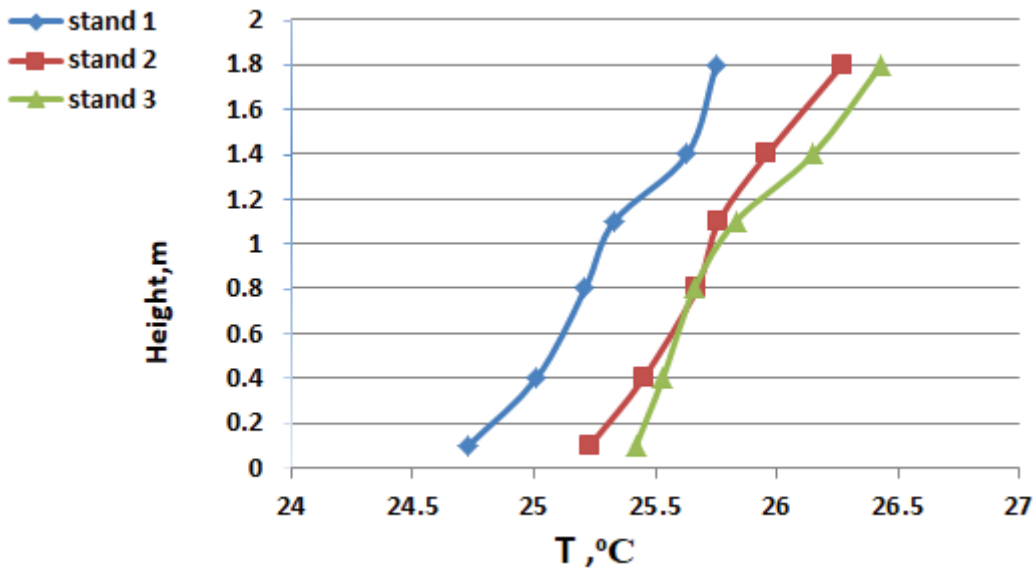


Figure 12. Temperature distribution (case II).

Table 7. Experimental measurements data for the case III

Height m	1 <sup>st</sup> stand	2 <sup>nd</sup> stand	3 <sup>rd</sup> stand
	Temperature °C	Temperature °C	Temperature °C
0.1	25.35	25.55	25.83
0.4	25.43	25.86	26.372
0.8	25.62	25.93	26.561
1.1	25.93	26.35	26.97
1.4	26.33	26.631	27.35
1.8	26.52	26.952	27.63

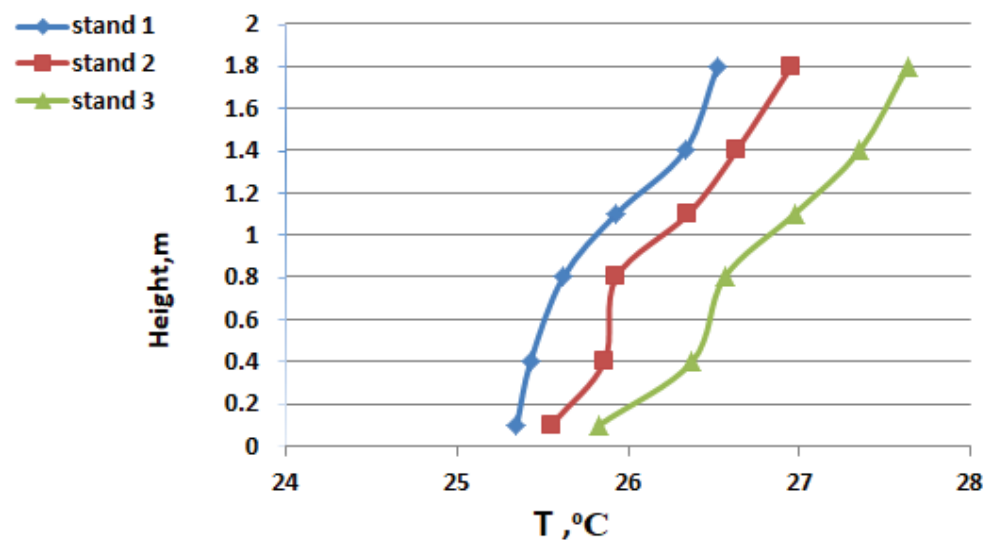


Figure 13. Temperature distribution (case III).

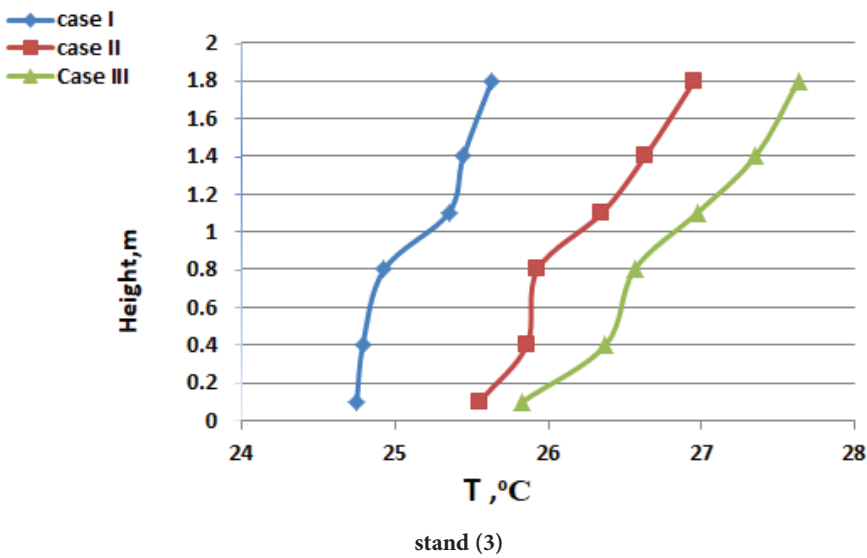
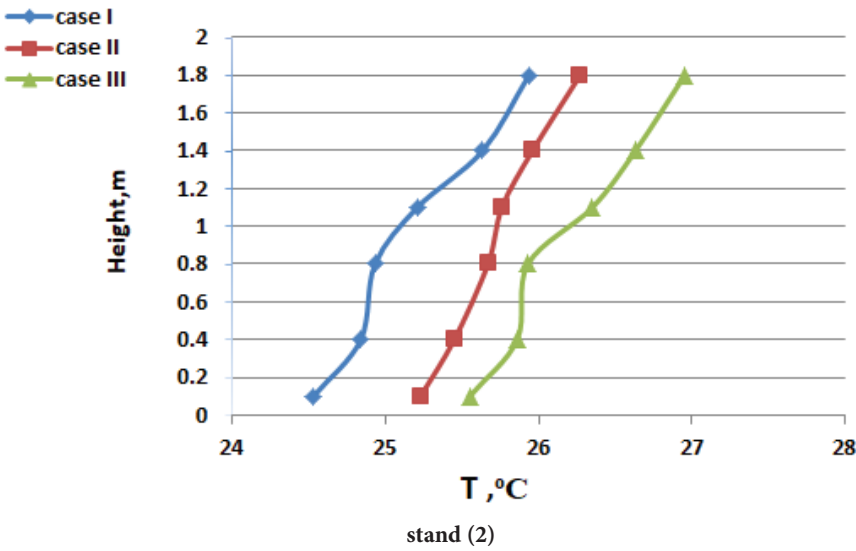
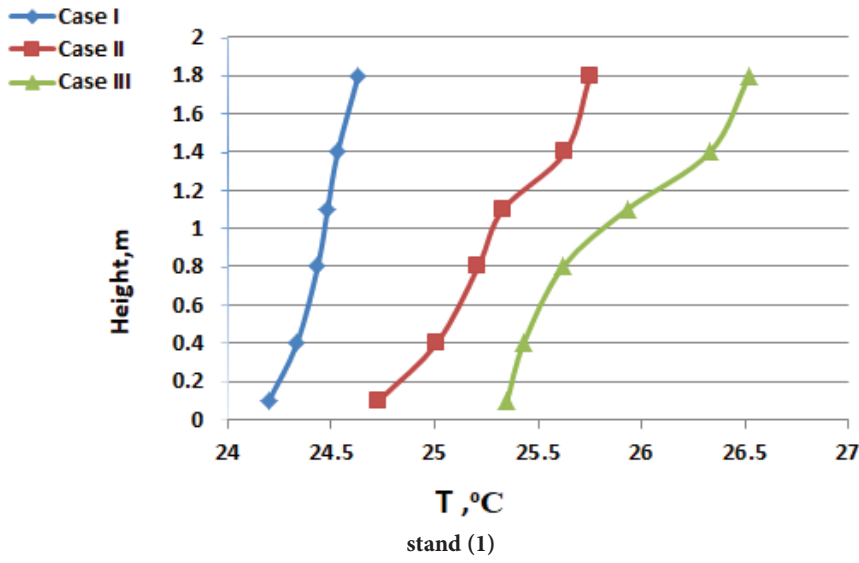


Figure 14. Temperature gradient with height for three cases (different occupants' density) for three stands.

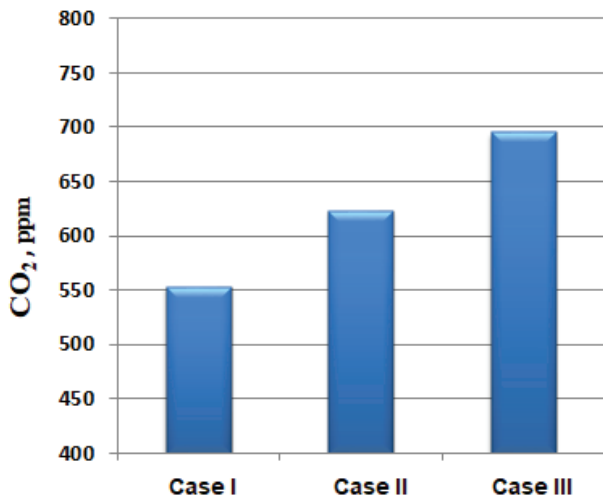


Figure 15. CO<sub>2</sub> concentration at different occupants’ density at (1.1 m).

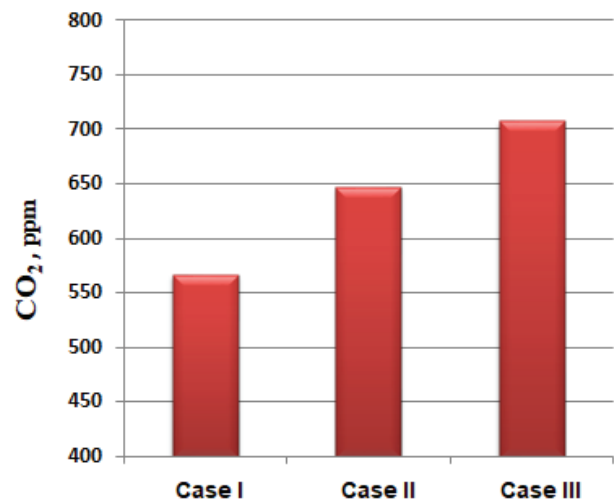


Figure 16. CO<sub>2</sub> concentration at different occupants’ density at (1.8 m).

altitude level. All three tests show differences in (CO<sub>2</sub>) concentration with different occupant density. The results indicate that the concentration of carbon dioxide (CO<sub>2</sub>) indoor the room increases with the increase in the number of persons (occupants’ density). In the first case, when there are two persons inside the rooms, we notice the concentration (CO<sub>2</sub>) in the breathing areas when sitting (1.1 m) and standing (1.8m) does not exceed (550 ppm) and this gives a good indicator of the air quality indoor the room. In the second case, when there were three persons in the room, the concentration of (CO<sub>2</sub>) in the two breathing areas (1.1 m) (1.8 m) exceeded (600 ppm), but the permissible and recommended limit of (650 ppm) was not exceeded, and this gives an acceptable indication of the air quality inside the room. Regarding the third case, when there are four persons, we notice that the (CO<sub>2</sub>) concentration has exceeded the (650 ppm) barrier, and therefore the room is not qualified to be there. The reason for the increase in the concentration of carbon dioxide (CO<sub>2</sub>) indoor the room is because the person gives a high concentration of carbon dioxide (40000-53000) at a rate

(6-15 l/min) [18]. To reach an ideal state and an acceptable concentration indoor the room when four persons are present, the designers need to increase the area of the room or increase the flow of air entering the room, which contains a concentration of (CO<sub>2</sub>) (400-450) ppm.

### Numerical Results

#### Analysis of temperature distribution

Figure (17 a) shows contours of temperature in the Y-plane at (Y = 1.1 m) around the occupant’s density when there are two persons indoor the office room (case-I). The average temperature around the occupants (25.418 °C), while the room’s lowest temperature was (24.639 °C). The room’s average temperature (excluding the inhaled temperature (34 to 36 °C) from the occupant’s nose and the temperature surrounding the simulated human body was around (26.075 °C). Figure (17 b) shows contours of temperature in the Y-plane at (Y = 1.8 m) around the occupant’s density when there are two persons inside the office room (case-I).

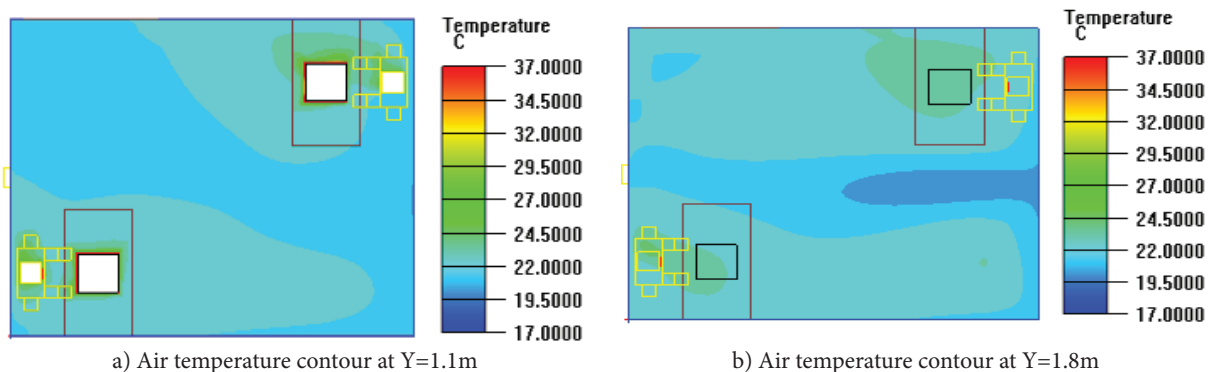


Figure 17. COntour of air the temperature in Y-plane (case-I).

Figure (18a) shows contours of temperature in the Y-plane at (Y=1.1 m) around the occupant's density when there are three persons indoor the office room (case- II). The average temperature around occupants was (26.603 °C), while the room's lowest temperature was (25.853 °C). The mean temperature in the office room (27.360 °C).

Figure (18 b) shows contours of temperature in Y-plane at (Y = 1.8 m) around the occupant's density when there are three persons indoor the office room (case- II).

Figure 19a shows contours of temperature in Y-plane (Y=1.1 m) around occupant's density of when there are four persons in the office room (case- III). The average temperature around the occupants (27.896 °C), while the room's lowest temperature was (27.160 °C). The mean temperature in the room (28.682 °C).

Figure 19b shows contours of temperature in the Y-plane at (Y = 1.8 m) around the occupant's density when there are four persons inside the office room (case- III).

The results showed an increase in the average room temperature and in the breathing area when the number of persons (occupants' density) increased indoor the room as a result of the heat generated by the human body (80 watts).

**Analysis of carbon dioxide concentrations (CO<sub>2</sub>)**

Figure 20a shows the (CO<sub>2</sub>) contours in the Y-plane at (Y=1.1 m) around the occupant's density when there are two persons indoor the office room (case-I). The minimum (CO<sub>2</sub>) in the office room was (542.831p.p.m). while the maximum (CO<sub>2</sub>) in the office room (596.009 p.p.m). Figure 20b shows the (CO<sub>2</sub>) contours in the Y-plane at (Y=1.8 m) around the occupant's density when there are two persons indoor the office room (case- I).

Figure 21a shows the (CO<sub>2</sub>) contours in the Y-plane at (Y=1.1 m) around the occupant's density when there are three persons indoor the office room (case- II). The minimum (CO<sub>2</sub>) in the office room was (610.46p.p.m). while the maximum (CO<sub>2</sub>) in the office room (664.773 p.p.m). Figure 21b shows the (CO<sub>2</sub>) contours in the Y-plane at (Y=1.8 m) around the occupant's density when there are three persons indoor the office room (case- II).

Figure 22a shows the (CO<sub>2</sub>) contours in the Y-plane at (Y=1.1 m) around the occupant's density when there are four persons indoor the office room (case- III). The minimum (CO<sub>2</sub>) in the office room was (684.729 p.p.m). while the maximum (CO<sub>2</sub>) in the office room (744.315 p.p.m). Figure 22b shows the (CO<sub>2</sub>) contours in the Y-plane at

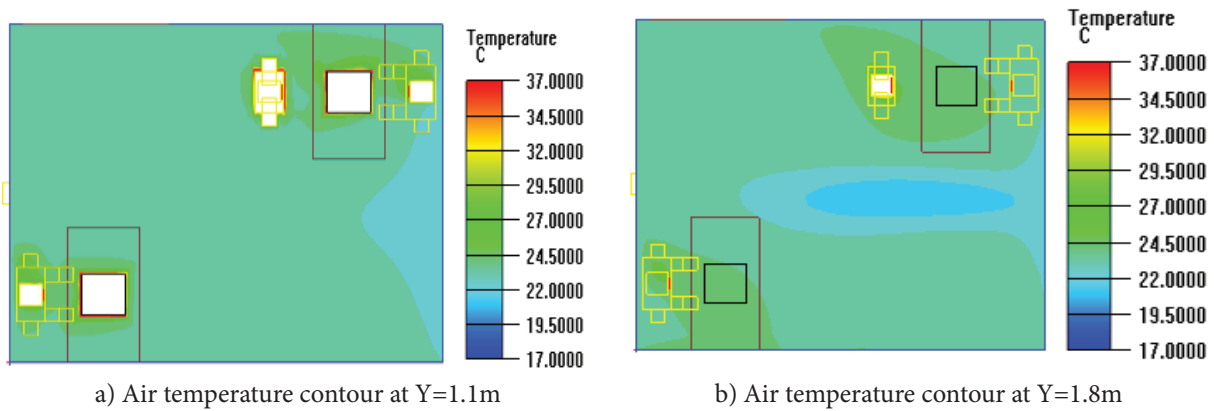


Figure 18. COntour of air the temperature in Y-plane (case- II).

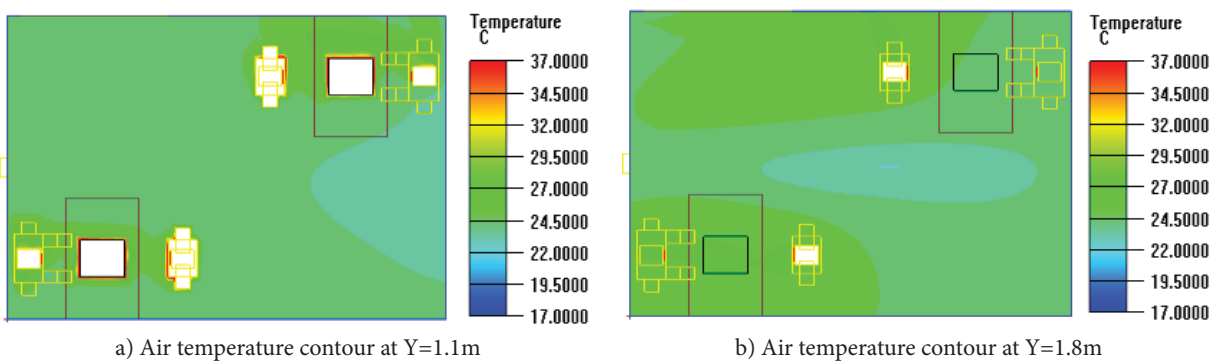


Figure 19. COntour of air temperature in Y-plane (case- III).

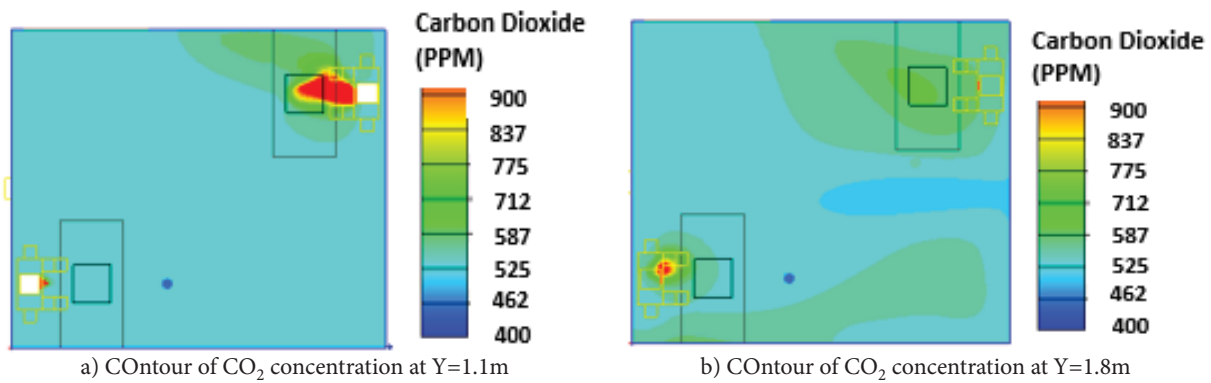


Figure 20. COntour of CO<sub>2</sub> concentration in Y-plane (case- I).

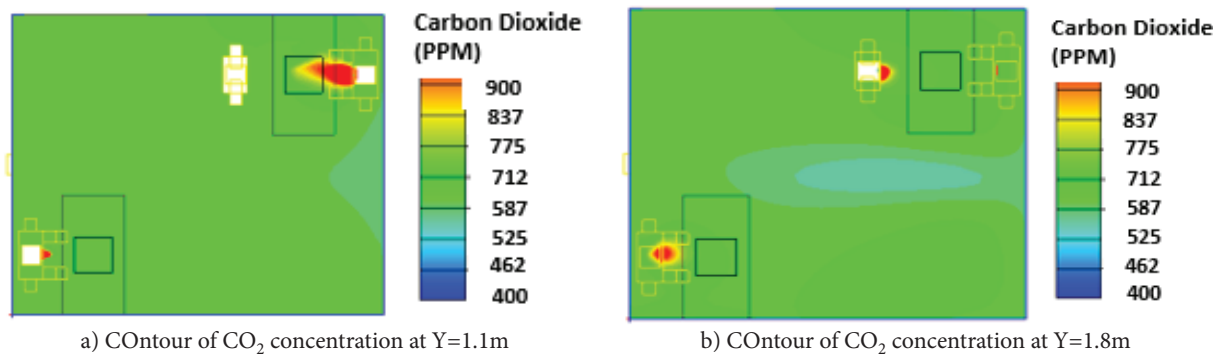


Figure 21. COntour of CO<sub>2</sub> concentration in Y-plane (case- II).

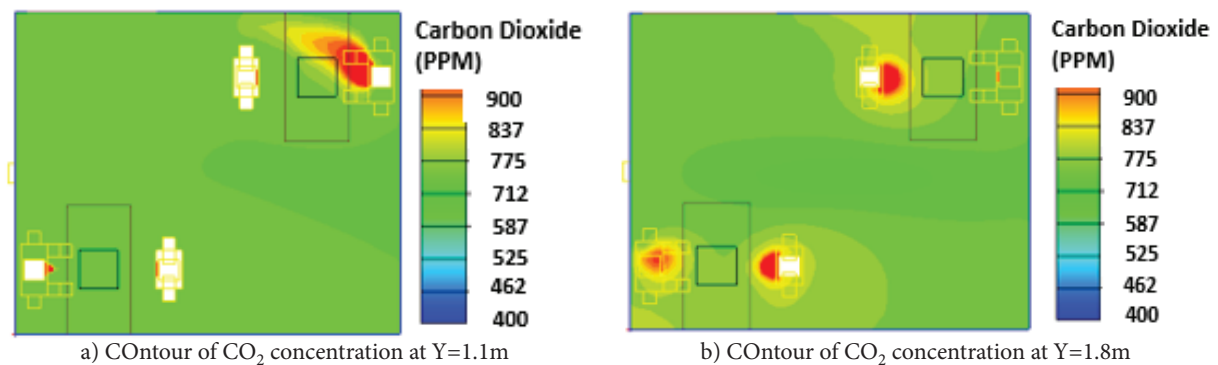


Figure 22. COntour of CO<sub>2</sub> concentration in Y-plane (case- III).

(Y=1.8 m) around the occupant’s density when there are four persons indoor the office room (case- II).

In all the cases studied (case-I to case- III), it was found that the concentration of carbon dioxide (CO<sub>2</sub>) increases with the increase in the number of person, due to the high concentration of carbon dioxide in human exhalation, which ranges (40000-53000 p.p.m), at a rate of (6-15 l /min)

[18]. Which affects the thermal comfort of persons indoor the office room.

**Quality of air and thermal level of comfort**

(PMV), (PPD), and (ADPI) are measures that provide information on thermal level of comfort and quality of air in occupied zoon, [20]. Figure 23 depicts the profiles of (PMV) for three distinct occupant densities. Noted that the

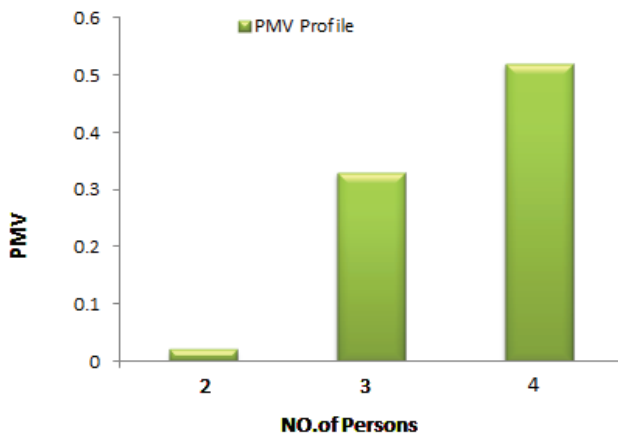


Figure 23. PMV profile for office room.

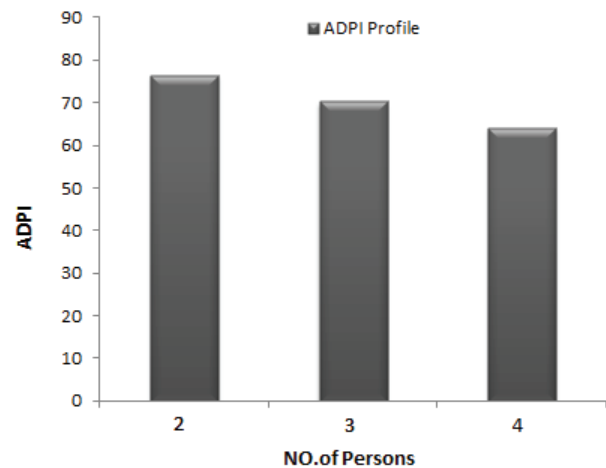


Figure 25. ADPI profile for office room.

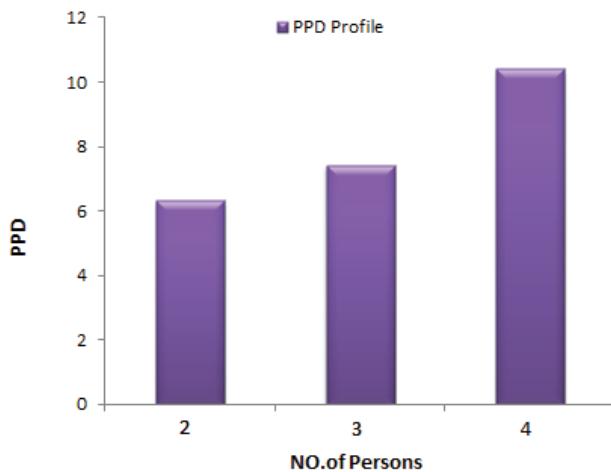


Figure 24. PPD profile for office room.

(PMV) values improve with the decrease in the number of person (occupants' density) converge with the comfort values defined by ASHRAE 2017 standard [21]. ( $-0.5 \leq PMV \leq 0.5$ ). At number of persons change from (2 persons to 4 persons) the (PMV) increase from (0.021 to 0.52) in office room (case-I to case-III).

Figure 24 showed the (PPD) profiles for three examples with varying occupant densities. Noted that the PPD values improve with the decrease in the number of persons in the office room and converge with the comfort values defined by ASHRAE 2017 standard (PPD=10%). At number of persons change from (2 persons to 4 persons) the (PPD) increase from (6.325 to 10.412).

An increase in (ADPI) % denotes occupant comfort; it is a factor used to predict the interior air circulation system. Figure 25 displays the percentage values of (ADPI), note that the (ADPI) increases in an office space when the occupant density falls.

## CONCLUSION

The current work investigates the numerical analysis and experimental testing of human thermal level of comfort and quality of air in an office environment utilizing a mixing ventilation) system in the Iraqi climate.

1. The average temperature around the occupants increased from (25.418 °C) to (27.896 °C) when the occupant's density increased from (2 to 4) persons.
2. Carbon dioxide concentration (CO<sub>2</sub>) increased from (569.42 ppm) to (714.522 ppm), when the number of occupant's density increased from (2 to 4) persons.
3. The area between heat sources has a minimum value for air quality due to the high temperature and carbon dioxide in this area
4. Reducing the number of persons in a room tends to improve thermal comfort indices (ADPI), (PPD) and (PMV).
5. By anticipating air flow patterns and thermal behavior for mixing ventilation (MV) equipment in simulated office environments, the model of turbulence (RNG, k-ε) gives the better consistency between numerical and experimental results in verification situations.
6. The mixing ventilation system does not give a large difference in temperature at the vertical height, but in general the temperature rises slightly when the vertical in the room ins increased.

## NOMENCLATURE

A	surface area, m <sup>2</sup> .
C <sub>p</sub>	specific heat, J/Kg.°C
K	turbulence kinetic energy
m.	air mass flowrate, Kg/s
P <sub>i,j</sub>	turbulence production due to viscous forces
P <sub>ij,k</sub>	influence of the buoyancy forces on turbulence

q	heat gain, W
Q	air supply flowrate. m <sup>3</sup> /s.
T	temperature, °C
u, v, w	Velocity component in x, y, and z-directions
x,y,z	a cartesian coordinate system's direction
ui,uj	Reynolds stresses

## Greek letters

$\Delta T_{hf}$	Temperature difference from head to foot level.
$\rho$	density of the air, kg/m <sup>3</sup>
$\varepsilon$	Efficiency
$\Delta T$	temperature difference
$\Phi_{i,j}$	pressure-strain correlation

## Abbreviations

ACH	air change per hour, 1/h
Amp.	ambient temperature. °C
ADPI	Air Distribution Performance Index
ASHRAE	American Society of Heating, Refrigeration, and Air Conditioning Engineers
CO <sub>2</sub>	Carbon dioxide
CFD	COmputational Fluid Dynamics
CO <sub>2</sub>	Carbon dioxide
CL	cooling load, W
MV	mixing ventilation
PPD	predicted percentage dissatisfied
PMV	predicted mean vote
PPM	Part Per Million
RSM	Reynolds Stress turbulence Model
RNG	Re-Normalization of Group
RNG	Re-Normalization Group
RH	relative humidity, %.
SBS	Sick of Building Syndrome

## Sub – Scripts

av	average
e	Exhaust Air
dr	design room
e	exit
ex	external
f	floor
hf	head to foot level.
l	overhead light
oe	occupants and equipment
i, j, k	In a Cartesian grid, the location of a point
o	Overhead light

## AUTHORSHIP CONTRIBUTIONS

Authors equally contributed to this work.

## DATA AVAILABILITY STATEMENT

The authors confirm that the data that supports the findings of this study are available within the article. Raw

data that support the finding of this study are available from the corresponding author, upon reasonable request.

## CONFLICT OF INTEREST

The author declared no potential conflicts of interest with respect to the research, authorship, and/or publication of this article.

## ETHICS

There are no ethical issues with the publication of this manuscript.

## REFERENCES

- [1] Wargocki P, Sundell J, Bischof W, Brundrett G, Fanger PO, Gyntelberg F, et al. Ventilation and health in non-industrial indoor environments: report from a European Multidisciplinary Scientific COnsensus Meeting (EUROVEN). *Indoor Air* 2002;12:113–128. [\[CrossRef\]](#)
- [2] Wargocki P, Djukanovic R. Simulations of the potential revenue from investment in improved indoor air quality in an office building. *ASHRAE Transactions* 2005;111.
- [3] Bluysen PM, de Oliveira Fernandes E, Groes L, Clausen G, Fanger PO, Valbjørn O, et al. European indoor air quality audit project in 56 office buildings. *Indoor Air* 1996;6:221–238. [\[CrossRef\]](#)
- [4] Saheb HA, Al-Amir QR. A comparative study of performance between two combined ventilation systems and their effect on indoor air quality and thermal comfort inside office rooms. *IOP Conference Series: Mater Sci Engineer* 2021;1095:012001. [\[CrossRef\]](#)
- [5] Awbi HB. *Ventilation Systems: Design and Performance*. Abingdon: Taylor and Francis; 2007. [\[CrossRef\]](#)
- [6] Reynders G, Saelens D. Numerical and experimental evaluation of ventilation in laboratories: A case study. Available at: file:///Users/kare2022/Downloads/Reynders,%20Saelens%20-%202011%20-%20NUMERICAL%20AND%20EXPERIMENTAL%20EVALUATION%20OF%20VENTILATION%20IN%20LABORATORIES%20A%20CASE%20STUDY.pdf. Accessed March 12, 2024.
- [7] Wang Z, Zhu Y, Wang F, Wang P, Shen C, Liu J, eds. *Proceedings of the 11th International Symposium on Heating, Ventilation and Air COnditioning (ISHVAC 2019): Volume I: Indoor and Outdoor Environment*. Berlin: Springer Nature; 2020. [\[CrossRef\]](#)
- [8] Xue K, Cao G, Liu M, Zhang Y, Pedersen C, Mathisen HM, et al. Experimental study on the effect of exhaust airflows on the surgical environment in an operating room with mixing ventilation. *J Build Engineer* 2020;32:101837. [\[CrossRef\]](#)

- [9] Shah Y, Kurelek JW, Peterson SD, Yarusevych S. Experimental investigation of indoor aerosol dispersion and accumulation in the context of COVID-19: Effects of masks and ventilation. *Physics Fluids* 2021;33:073315. [\[CrossRef\]](#)
- [10] ASHRAE. *Fundamentals Handbook*. 2013.
- [11] ASHRAE. *HVAC Systems and Equipment (SI). Panel heating and cooling*; 2012.
- [12] ASHRAE. *Standard 55, Thermal environmental conditions for human occupancy*. Atlanta; 2010.
- [13] Awbi HB. Ventilation for good indoor air quality and energy efficiency. *Energy Procedia* 2017;112:277–286. [\[CrossRef\]](#)
- [14] Shbeeb AA, Mahdi AA, Hussein AK. Effects of supply diffuser shape on air age and human comfort in an office with displacement ventilation and chilled ceiling system in hot and dry climate. *IOP Conference Series: Mater Sci Engineer* 2021;1067:012089. [\[CrossRef\]](#)
- [15] Fluent Inc. *Fluent 6.3.26 User's Guide*. 2006.
- [16] Hussein JM, Farooq AH, Al-Amir QR, Hameed KH, Khafaji SOW. Entropy generation analysis of a natural convection inside a sinusoidal enclosure with different shapes of cylinders. *Front Heat Mass Transf* 2019;12:22. [\[CrossRef\]](#)
- [17] Mahdi AA, Jasim ZH. Experimental and numerical study of air flow diffusion and contaminants circulation in room ventilation related with Iraqi climate. *Int J Mech Engineer Appl* 2016;4:24–42. [\[CrossRef\]](#)
- [18] Bhagat RK, Wykes MD, Dalziel SB, Linden PF. Effects of ventilation on the indoor spread of COVID-19. *J Fluid Mech* 2020;903. [\[CrossRef\]](#)
- [19] Fluent ANSYS. *ANSYS fluent theory guide 15.0*. Canonsburg, PA: ANSYS; 2013. p. 33.
- [20] Awbi H. *Ventilation of Buildings*. 2nd ed. Abingdon: Taylor & Francis; 2008.
- [21] ASHRAE. *Fundamentals Handbook*. 2017.